HHS Public Access

Author manuscript

Blood Cells Mol Dis. Author manuscript; available in PMC 2022 March 01.

Published in final edited form as:

Blood Cells Mol Dis. 2021 March ; 87: 102524. doi:10.1016/j.bcmd.2020.102524.

Rasa3 Regulates Stage-Specific Cell Cycle Progression In Murine Erythropoiesis

Elena C. Brindley[1,2], **Julien Papoin**[2], **Lauren Kennedy**[2], **Raymond F. Robledo**[3], **Steven L. Ciciotte**[3], **Theodosia A. Kalfa**[4], **Luanne L. Peters**[3,*], **Lionel Blanc**[1,2,*]

[1]Department of Molecular Medicine and Pediatrics, Zucker School of Medicine at Hofstra/Northwell, Hempstead, NY 11549, USA

[2]Laboratory of Developmental Erythropoiesis, Les Nelkin Memorial Laboratory of Pediatric Oncology, Institute of Molecular Medicine, The Feinstein Institutes for Medical Research, Manhasset, NY 11030, USA

[3]The Jackson Laboratory, Bar Harbor, ME 04672, USA

[4]Department of Pediatrics, Cincinnati Children's Hospital Medical Center, Cincinnati, OH 05229

Abstract

Inherited bone marrow failure syndromes (IBMFS) are heterogeneous disorders characterized by dysregulated hematopoiesis in various lineages, developmental anomalies, and predisposition to malignancy. The *scat* (severe combined anemia and thrombocytopenia) mouse model is a model of IBMFS with a phenotype of pancytopenia cycling through crises and remission. *Scat* carries an autosomal recessive missense mutation in *Rasa3* that results in RASA3 mislocalization and loss of function. RASA3 functions as a Ras-GTPase activating protein (GAP), and its loss of function in *scat* results in increased erythroid RAS activity and reactive oxygen species (ROS) and altered erythroid cell cycle progression, culminating in delayed terminal erythroid differentiation. Here we sought to further resolve the erythroid cell cycle defect in *scat* through e*x vivo* flow cytometric analyses. These studies revealed a specific G0/G1 accumulation in *scat* bone marrow (BM) polychromatophilic erythroblasts and *scat* BM Ter119^{-}/c-KIT^{+}/CD71$^{lo/med}$ progenitors, with no changes evident in equivalent *scat* spleen populations. Systematic analyses of RNAseq data from megakaryocyte-erythroid progenitors (MEPs) in *scat* crisis vs. *scat* partial remission reveal altered expression of genes involved in the G1-S checkpoint. Together, these data indicate a precise,

Correspondence: Lionel Blanc, PhD, Laboratory of Developmental Erythropoiesis, Les Nelkin Memorial Laboratory of Pediatric Oncology, Institute of Molecular Medicine, The Feinstein Institutes for Medical Research, 350 Community Drive, Manhasset, NY 11030, Tel: (516)-562-1507, Fax: (516)-562-1599, Lblanc@northwell.edu.

*Co-senior authors.

Authorship

ECB designed, performed, and analyzed experiments and wrote the manuscript. JP, LK, RFR, SLC, performed and analyzed experiments. TAK, LLP and LB designed the project, advised experiments and analysis and edited the manuscript.

Declaration of Competing Interests

The authors have no conflicts of interest to report.

biphasic role for RASA3 in regulating the cell cycle during erythropoiesis with relevance to hematopoietic disease progression.

Keywords

erythropoiesis; cell cycle; RAS signaling; RAS-GAPs; inherited bone marrow failure

Introduction

Anemia affects approximately 25% of the global population and is associated with poor clinical outcomes and decreased quality of life [1]. Anemia is caused by decreased erythrocyte production, or increased erythrocyte destruction. Erythropoiesis in the bone marrow of a healthy individual produces 2 million erythrocytes every second. This high erythroid output ensures sufficient tissue oxygenation and is maintained by tight regulation of erythroid proliferation and differentiation. Erythroid differentiation is a complex process regulated at multiple levels [2]. Erythropoiesis is intimately linked to cell cycle progression throughout this dynamic process. Indeed, the transition from the erythroid progenitor stages to the precursor stages and the accompanying commitment to terminal differentiation coincides with downregulation of the cell cycle inhibitor $p57^{kip2}$ and is dependent upon S-phase to allow chromatin access for normal erythroid gene expression changes [3, 4]. Further, EKLF-mediated cell cycle exit is required for enucleation, allowing reticulocyte formation at the conclusion of terminal differentiation [5]. During normal murine erythropoiesis, the earliest erythroid lineage-committed progenitors, burst forming unit-erythroid (BFU-E), proliferate slowly. They give rise to highly cycling colony forming unit-erythroid (CFU-E) progenitors, then to the highly cycling earliest precursors of terminal erythroid differentiation, the proerythroblasts (ProEB) [6, 7]. Cells remain actively cycling through the basophilic (Baso) and polychromatophilic (Poly) erythroblast stages. At the transition to the orthochromatic erythroblast (Ortho) stage, there is final G0/G1 accumulation and cell cycle exit in preparation for enucleation [3]. Erythroid cell cycle dysregulation can contributes to ineffective erythropoiesis and resulting anemia in various disease contexts, including inherited bone marrow failure syndromes (IBMFS), which are a heterogeneous group of diseases characterized by dysregulation of one or more hematopoietic lineages, developmental anomalies, and predisposition to cancer [8–12]. Targeted alteration of cell cycle regulation is emerging as a therapeutic strategy for such disorders in both murine and human models [13, 14].

The *scat* (severe combined anemia and thrombocytopenia) mouse model is a model of IBMFS that carries an autosomal recessively inherited missense (G125V) mutation in *Rasa3*, resulting in mislocalization and loss of function of RAS-GTPase activating protein (GAP) RASA3 [15]. *Scat* mice cycle through crises characterized by hypocellular bone marrow and pancytopenia, then remissions during which bone marrow, hematologic parameters, and physical appearance normalize. *Scat* mice also manifest a specific delay in late terminal erythroid differentiation [15]. During crisis episodes, we previously identified a qualitative cell cycle defect of G0/G1 accumulation in late erythroblasts that aligned with the delay in terminal erythroid differentiation [16].

Here, we sought to resolve and quantify this defect during erythropoiesis to elucidate a more specific role for RASA3 in regulating the erythroid cell cycle with implications for diseases with disordered erythropoiesis such as IBMFS.

Methods

Mice

All protocols were performed according to National Institutes of Health animal care guidelines, as approved and enforced by the Institutional Animal Care and Use Committees at Northwell Health. The *scat* colony was maintained by interbreeding of heterozygous (*scat*/+) mice. *Scat* mice carry an autosomal recessive missense (G125V) mutation in the *Rasa3* gene, co-isogenic on the BALB/cBy background. Analyses of offspring (+/+ or *scat*/+ versus *scat*/*scat)* was performed at approximately P21, corresponding to the age of the second crisis event in homozygous mutant *scat* mice. Animals in crisis were identified by overall appearance and complete blood counts as described in [15].

Flow Cytometry

Isolation of erythroid cell populations from bone marrow and spleen.—The bone marrow of hindlimb bones (2 femurs and 2 tibiae per mouse) was harvested by flushing with a 26G syringe, pipet homogenized, and filtered (70μm) in phosphate buffered saline (PBS), 0.5% (weight/volume) bovine serum albumin (BSA), 2mM Ethylenediaminetetraacetic acid (EDTA). Whole spleens were harvested, pestle homogenized, and filtered in PBS/0.5% BSA only. Both bone marrow and spleen were CD45-depleted and/or Lineage depleted by magnetic microbead (Miltenyi Biotec # 130-052-301; 130-090-858) according to the manufacturer's protocol to enrich for erythroblasts or hematopoietic stem and progenitor cells (HSPCs), respectively.

Identification of hematopoietic and erythroid progenitors.—Following Lineage depletion (Miltenyi Biotec #130-090-858) including depletion of cells expressing CD5, CD45R (B220), CD11b, Ly-6G/C, and Ter119, Ter119 negativity was used to confirm lineage depletion, and progenitor populations were monitored by flow cytometry using a cocktail of Ter119 APC-Cy7-conjugated (BD Bioscience #560509, clone Ter119), c-KIT APC-conjugated (BioLegend #135108, clone ACK2), and anti-CD71 FITC-conjugated (BD Bioscience #553266, clone C2), gated based on [17].

Identification of erythroid precursors.—Following CD45-depletion, terminal erythropoiesis was monitored by flow cytometry using a cocktail of Ter119 APC-Cy7-conjugated (BD Bioscience #560509), anti-CD71 FITC-conjugated (BD Bioscience #553266, clone C2), gated based on [18].

Cell cycle analyses.—CD45-depleted or Lineage-depleted cells were incubated at 1 million per mL ($CD45^-$ precursors) or proportionally uniform cell concentrations based on cell number availability (Lin^- progenitors) in IMDM, 20% (volume/volume) fetal bovine serum (FBS), 2U/mL clinical grade EPO (Procrit) with the addition of 10μM EdU for 2 hours (precursors) or 1 hour (progenitors). Cells were then harvested, washed in PBS/0.5%

BSA, stained for surface markers as described above, and carried through Click-iT EdU-Pacific Blue kit fixation, permeabilization, and click chemistry reaction according to manufacturer's protocol (LifeTechnologies # C10636). Cells were then washed in PBS/0.5%BSA, suspended in PI/RNase staining buffer (BD #550825) for 15 minutes at room temperature, and analyzed on the BD LSR Fortessa. Data were analyzed using FCS Express 6 software.

Reactome analyses of RNAseq data

RNAseq was performed in our previous study [19]. RNAseq data obtained from stem and myeloid progenitors (SMP; Lin^{-}/c-KIT^{+}/CD16/32^{lo}/$CD34^{+}$) and megakaryocyte-erythroid progenitors (MEP; Lin^{-}/c-KIT^{+}/CD16/32^{-}/$CD34^{-}$) in *scat* crisis, *scat* partial remission (based on red cell counts, hemoglobin, and hematocrit levels intermediate to severe crisis and complete remission [19]), and WT mice was processed following the Jackson Laboratory's Computer Science group's Civet Single-end RNAseq Analysis Pipeline (https://github.com/TheJacksonLaboratory/civet/) followed by normalization and differential expression analysis with DESeq2 [20]. The SMP population was isolated as described due to the minimal expression of Sca-1 on the BALB/cBy background [21]. This data set was further systematically analyzed using the Reactome pathway database data analysis tool (https://reactome.org/) [22] including "project to human" and "include interactor" options, comparing pathway enrichment in sets of two-fold up and downregulated genes in SMP and MEP of bone marrow and spleen from *scat* crisis vs. wild type (WT, +/+) and *scat* crisis vs. *scat* partial remission, elucidating the top 5 enriched pathways in each group, and identifying all enriched cell cycle pathways across groups.

Data Availability.—RNAseq data were submitted from our previous study [19] to Gene Expression Omnibus (https://www.ncbi.nlm.nih.gov/geo/) with accession number GSE148821.

Statistics

All statistical analyses were performed using GraphPad Prism 8 (unpaired t-test, ANOVA with Tukey's multiple comparison or non-parametric equivalent for fold change analyses) with $p<0.05$ considered significant.

Results

A specific late erythroblast population in *scat* bone marrow, but not spleen, demonstrates G0/G1 accumulation.

We examined population-specific cell cycle progression in *scat* vs WT erythroblasts using *ex vivo* incubation with nucleoside analog EdU, DNA dye propidium iodide (PI), and modified surface markers of erythroid differentiation. The most accurate way to monitor and quantify terminal erythroid differentiation relies on the use of Ter119, CD44 and FSC as markers [23]. However, we noticed incompatibility of the staining with the fixation and permeabilization steps required for quantifiable two-dimensional cell cycle analyses [16]. We therefore used Ter119, transferrin receptor (CD71), and FSC, as previously published [18]. This method offers resolution of terminal erythropoiesis through gating $CD71^{hi}$/

TER-119^{med} as Proerythroblasts (ProEB), and further gating Ter119^{+} with decreasing CD71 expression and cell size as EryA (late ProEB to Basophilic), EryB (late Basophilic, Polychromatophilic, and Orthochromatic) and EryC (reticulocytes and erythrocytes), respectively. We compared the cell cycle progression of these populations in *scat* vs. WT BM and spleen and identified trends towards G0/1 accumulation and decreased cell cycle progression in *scat* EryA and EryB (Figure 1A–C).

While we were able to quantify cell cycle progression of populations by these markers, the heterogeneity of the EryA/B/C populations was evident by the appearance of dual cell cycle profiles within a single population (Figure 1B–C). Transitions in the EryA-B-C gating scheme are unidimensional, with the EryA-B transition characterized primarily by decreasing cell size, and the EryBC transition characterized by decreasing CD71 expression (Figure 1A). In addition, this gating method has mostly been used in whether in vivo or ex vivo studies of erythropoiesis using the fetal liver system. A recent study demonstrated dynamic changes of murine erythropoiesis during the neonatal period [24]. Therefore, we hypothesized that the trends observed in the differences in the cell cycle between WT and *scat* might be biologically significant but masked by the gating strategy. Using the same markers, we gated on six populations (I-VI) along the EryA/B/C pattern, with the goal to obtain higher resolution of simultaneous cell size and CD71 changes, and thus higher resolution of population cycling (Figure 2A). First, we quantified and compared normal cell cycle progression in WT bone marrow and spleen-derived erythroblast populations by both methods and found that we could indeed resolve the EryA population into populations I, II, and III, and the EryB population into population IV and V, with the transition from IV to V representing a key point of physiological G0/G1 accumulation towards the end of terminal differentiation (Figure 2B).

We then compared WT and *scat* populations I-V cell cycling and identified a 2-fold G0/G1 accumulation and decreased cell cycle progression specifically in *scat* BM population IV, with no changes evident in the spleen (Figure 3A–C). The overall pattern of differentiation stage and cell cycle progression is preserved in *scat* BM, but the relationship of the cell cycle profile of population IV with that of neighboring populations is disrupted, highlighting the specificity and magnitude of the phenotype (Figure S1). Together, these results support and refine our previous cell cycle findings and identify RASA3 as a stage-specific regulator of murine erythroid cell cycle progression.

Hematopoietic progenitors (HPCs) in *scat* bone marrow, but not spleen, demonstrate G0/1 accumulation

The defect in cell cycle in population IV in *scat* appears to represent the culmination of erythroid failure, with subsequent orthochromatic erythroblasts, reticulocytes, and erythrocytes (population V, VI, or EryC) showing incomplete maturation and membrane fragmentation [15]. Erythropoietic cell cycle control has been characterized as dual coordination of early and late cell cycle entry and exit [3–5], respectively, and erythroid progenitors are emerging as key modifiable stages of erythroid differentiation [25]. We therefore wanted to explore if RASA3 also played a role in regulating cell cycle progression at the erythroid progenitor stages in the *scat* mouse model. However, methods identifying

erythroid progenitors in the mouse have been inconsistent across studies and tissues, with varying degrees of erythroid and stage specificity [4, 17]. Therefore, we chose to utilize a gating scheme that best allowed us to combine population gating with cell cycle analyses in order to determine if *scat* cell cycle progression is altered prior to terminal erythroid differentiation.

Lineage-depleted BM and spleen cells were stained for c-KIT, CD71, and Ter119 to verify lineage depletion. Lin^{-}/c-KIT+ cells were gated by increasing CD71 expression (lo, med, hi) marking increasing differentiation as previously published [17]. Sca-1 was not included as BALB/cBy mice express negligible levels of this marker [21]. The Lin^{-}/c-KIT^{+}/$CD71^{hi}$ population represents late CFU-E/early proerythroblasts, while earlier $CD71^{lo}$ and $CD71^{med}$ populations are more heterogeneous and likely represent a combination of multipotent progenitors and more fate-restricted progenitors that we will refer to simply as hematopoietic progenitor cells (HPCs).

We first analyzed HPC population frequencies and found that *scat* has decreased or trends toward decreased HPCs and increased or trends toward increased $CD71^{Hi}$ compared to WT in both BM and spleen, suggesting a dysregulated erythroid stress response at the HPC stage (Figure 4A). In our cell cycle analyses, *scat* BM-derived HPC populations show consistent 10–15% G0/G1 accumulation and decreased cell cycle progression that normalizes in the $CD71^{Hi}$ population. *Scat* spleen progenitor populations maintained normal cell cycle progression (Figure 4B–C). Importantly, the WT Lin^{-}/c-KIT^{+} populations from $CD71^{lo}$ to $CD71^{hi}$ in both BM and spleen demonstrate cell cycle profiles that match previously published cell cycle analyses of the BFU-E (30% S-phase) to CFU-E (75% S-phase) progression, supporting our method and findings [6, 7]. Together, these results indicate a role for RASA3 in regulating the cell cycle in BM HPCs prior to and similar to its role in late terminal erythroid differentiation.

Systematic RNAseq analysis identifies potential cell cycle-related mechanisms in *scat* disease progression

For molecular insight into how loss of RASA3 function alters hematopoiesis and erythropoiesis in the bone marrow and spleen, we previously obtained RNA-sequencing data from bone marrow and spleen-derived sorted “stem and myeloid progenitors” (SMP) and megakaryocyte-erythroid progenitors (MEP) in wild type, *scat* crisis, and *scat* partial remission mice, providing a resource for parsing apart mechanisms of *scat* disease in a population-, tissue-, and disease-stage-specific manner [19]. Initial Gene Ontology analyses demonstrated enriched differential expression of cell cycle and calcium channel related genes in *scat* vs. WT [19]. After confirmation of a cell cycle phenotype in *scat* HPCs, further analyses of this RNAseq data utilizing the Reactome pathway database yielded cell-cycle related pathways of interest in *scat* disease progression. Genes that were two-fold or more differentially expressed in SMP or MEP populations in bone marrow and spleen between *scat* crisis and WT or *scat* crisis and *scat* partial remission were analyzed for the top 5 associated Reactome pathways, including conversion of murine genes to their human equivalents and molecular interactions form the IntAct database (Tables 1–2). “Signaling by MAPK mutants” appeared across several comparisons, providing an indirect validation of

this approach given the role of RASA3 as a regulator of RAS and previously published evidence of increased active RAS in *scat* peripheral blood [15]. Within the top 5 pathways for each comparison, a single cell-cycle pathway emerged only from the list of genes upregulated in *scat* crisis vs. *scat* partial remission in bone marrow MEP, namely "TP53 regulates transcription of additional cell cycle genes whose exact role in the p53 pathway remain uncertain." This suggests that RASA3 regulates known RASp53 mediated G1-S cell cycle progression and that this mechanism associates with crisis progression within *scat* BM.

Additional cell cycle pathways that emerged with $p<0.05$ that were not included in the top five per comparison further suggest a G1-S checkpoint defect in disease progression shared by the bone marrow and spleen MEP. Both bone marrow and spleen MEP *scat* crisis vs. *scat* partial remission demonstrated "evasion of oxidative stress/oncogene induced senescence due to $p14^{ARF}$ defects" enriched in downregulated genes and "aberrant regulation of mitotic G1-S transition in cancer due to RB1 defects" and "defective binding of RB1 mutants to E2F1, (E2F2, E2F3)" enriched in upregulated genes (Table 3). Finally, to investigate the mechanisms underlying the MEP G_1-S checkpoint defects, we overlaid the list of genes downregulated in bone marrow (24 genes) and spleen (42 genes) MEP *scat* crisis vs. *scat* partial remission and identified 5 shared genes (*Ifitm1, Mycn, Rab44, Slc22a3, and St8sia6*) that were enriched for "evasion of oxidative stress/oncogene induced senescence due to $p14^{ARF}$ defects" in their top three pathways. Similarly, we overlaid the list of genes upregulated in bone marrow (20 genes) and spleen (32 genes) MEP *scat* crisis vs. *scat* partial remission and identified 9 genes (*Cdkn1c, Cntn3, Homer2, Lama5, Pcsk6, Spry1, Tmem88b, 0610040J01Rik, 2510009E07Rik*) that were enriched for "mitotic G_1-S transition dysregulation in cancer due to RB1 defects" and "defective binding of RB1 mutants to E2F1, E2F2, E2F3" in their top three pathways. Complete gene lists are presented in Tables S1 and S2.

Discussion

This work resolved and quantified the erythroid cell cycle defect resulting from RASA3 loss of function in *scat*. Overall, the identification of a G0/1 accumulation in *scat* BM HPCs that normalizes by the CFU-E stage and remanifests at the polychromatophilic stage suggests a precise, biphasic role for RASA3 in erythropoiesis. Further resolution of $Ter119^{+}$ erythroblast populations by CD71 and cell size allowed analysis of uniformly cycling erythroblasts and identification of a specific late erythroblast population most affected in *scat* that aligns with the observed delay in erythroid differentiation. Our identification of a specific progenitor population was limited to Lin^{-}/c-KIT^{+}/$CD71^{lo/med}$ HPCs given the less established surface markers for murine erythroid progenitors. However, this data represents the first characterization of erythroid progenitor cell cycle status in *scat*, and these populations play a key role in the erythroid stress response that is part of *scat* disease progression.

These data raise questions of how loss of RASA3 function can cause this stage-specific cell cycle dysregulation, and how this dysregulation can contribute to anemia. RAS signaling pathways are known to influence expression and activity of D, E, and A-type cyclins, and cell cycle inhibitors p27, p53, and p21, and these genes display stage-specific expression in

erythropoiesis [4, 26]. Given the role of RASA3 as a RAS-GAP, we hypothesized that dysregulation of stage-specific RAS-mediated cell cycle control networks during hematopoiesis contribute to the cell cycle defect in *scat*. RNAseq analyses demonstrated that overall alterations in cell cycle-related genes were focused within the MEP population of *scat* BM and spleen at varying stages of disease (crisis vs. partial remission), most prominent in the bone marrow, aligning with our *ex vivo* cell cycle analyses. This suggests that, at least at the transcriptional level, there is onset of G1-S checkpoint dysregulation at the MEP stage that uniquely correlates with crisis progression in *scat* in both the bone marrow and spleen. The identified cell cycle processes disrupted in *scat* include uncharacterized targets of p53, evasion of oxidative stress/oncogene induced senescence due to $p14^{ARF}$ defects, defective G_1-S transition due to RB1 and E2F defects, all highlighting the G_1-S checkpoint. Notable among the gene signatures contributing to these findings is the upregulation of *Cdkn1c*, encoding cell cycle inhibitor p57, with *scat* disease progression in bone marrow and spleen MEP, and the implication of E2F2 binding by RB1, as both have specific erythroid relevance. In mice, the commitment to terminal erythroid differentiation requires downregulation of p57 to facilitate S-phase dependent transcriptional changes, and modulation of p57 by corticosteroids is an emerging mechanism of increasing erythroid output in IBMFS [3, 13, 14]. E2F1 and E2F2 have been demonstrated as critical mediators of cell cycle regulation in murine hematopoiesis, specifically in progenitor S-phase progression, with E2F2 also an important regulator of erythroid cell cycle regulation and size control in differentiation [27]. Previous work in *scat* also identified increases in reactive oxygen species (ROS) and decreased apoptosis in various erythroid populations compared to WT [16]. $p14^{ARF}$ has been characterized as a key E2F1 target gene and inducer of senescence in response to various stressors [28]. Changes in evasion of senescence induced by increased ROS or RAS signaling in *scat* erythroblasts may reconcile their decreased apoptosis with anemia, as aberrant survival of defective erythroblasts still results in decreased functional erythroid output. Further investigation of this gene signature, along with obtaining comparable data from later erythroblast populations, may yield insights into how RASA3 regulates the erythroid cell cycle throughout differentiation, along with general mechanisms of erythroid cell cycle regulation in health and disease.

Dysregulated cell cycle progression of hematopoietic progenitor cells and erythroblasts is implicated in anemia in various contexts. Myelodysplastic syndrome (MDS) can be characterized by genetic defects in cell cycle regulators contributing to ineffective erythropoiesis, congenital dyserythropoietic anemias (CDAs) occur with defects in cell division machinery, and the pathogenesis of Diamond-Blackfan anemia (DBA) involves upregulation of p53, and dysregulation of cell cycle inhibitors is associated with therapeutic response in DBA patients [9, 10, 12, 13, 29, 30]. Given this context, we hypothesize that the cell cycle defect characterized here contributes to the anemia of *scat* through disruption of erythroid differentiation. Future mechanistic studies verifying specific RAS pathways and cell cycle regulators altered in *scat* are needed and can now be directed to the populations of interest identified here.

Downregulated genes in BM MEP *scat* crisis vs WT were also uniquely enriched for the cell cycle-related interaction of PHLDA1 and AURKA, or pleckstrin homology-like domain family A member 1 and Aurora A kinase. Aurora A kinase normally contributes to

centrosome organization in G_2/M phases of the cell cycle but is overexpressed in several malignancies. PHLDA1 is both a substrate and negative regulator of AURKA, with PHLDA1 and AURKA co-regulating cell cycle processes in a feedback loop [31, 32]. As the only G_2/M related process identified, the biological significance of this finding remains unknown.

Given our hypothesis that cell cycle dysregulation contributes to the anemia in *scat*, the limited number of cell cycle pathways that emerged from our RNAseq may seem surprising. However, the populations from which this RNAseq data was obtained, while sorted, retained some heterogeneity in differentiation stage and disease stage and, as early progenitors, have abundant transcriptional potential. Therefore, some pathway searches, especially in the SMP population, were dominated by immune system-related terms. Additionally, the gene expression changes between *scat* crisis vs. *scat* partial remission are likely subtle as they represent disease progression within a single genotype. The combination of unbiased searches for the top five pathways from a given gene list and biased searches for significant enrichment of cell cycle pathways across gene lists hopes to maximize the impact of information extracted from this data despite these challenges. The fact that both approaches similarly emphasized cell cycle changes in the MEP population in the bone marrow, and the alignment of this conclusion with our *ex vivo* cell cycle analyses supports the utility of this approach. Further, key cell cycle regulatory events occur at both the transcriptional and post-translational levels, with post-translational modifications such as phosphorylation and ubiquitination offering rapid induction of cell cycle changes [33, 34]. Therefore, transcriptional read-out of cell cycle regulators, while informative, is an incomplete picture of real-time cell cycle regulation in *scat* disease stages.

Finally, this data also raises important questions about differential regulation of BM and spleen erythropoiesis in general physiology, stress, and specifically in *scat* disease progression. Through approximately 2 months of age, the spleen is an erythropoietic organ in the mouse, performing a remnant developmental type of “stress” erythropoiesis while homeostatic BM erythropoiesis continues to be established [24]. In this work, mice were examined at approximately P21, when the second hematopoietic crisis occurs in *scat* [15]. In *scat* crisis, BM erythropoiesis fails, and the spleen becomes the primary erythropoietic organ, temporarily compensating and inducing reticulocytosis, then eventually failing as well. Therefore, analysis of WT vs. *scat* at P21 offers fair comparison of bone marrows performing homeostatic erythropoiesis (normal in WT vs. failed in *scat*) and spleens performing stress erythropoiesis (developmental in WT and disease-driven in *scat*), though these are likely distinct stress responses. However, comparison of phenotypes in *scat* BM versus *scat* spleen is complicated by the fact that these tissues are performing homeostatic versus stress erythropoiesis, respectively. Therefore, differences in the cell cycle phenotype of *scat* BM versus *scat* spleen (G0/1 accumulation identified in *scat* BM but not in *scat* spleen) may be attributable to the fact that RASA3 may function differently in the pathways and processes of homeostatic versus stress erythropoiesis, which are known to have distinct signaling and cell cycle requirements [35, 36]. Alternatively, similar mechanisms of erythroid failure due to loss of RASA3 may occur sequentially in the bone marrow, then the spleen, demonstrating different phenotypes at a single timepoint of analysis. Similar gene expression signatures with disease progression in *scat* BM and spleen MEP populations

support the later, at least at the MEP stage. The role of RASA3 in the microenvironments of the BM and spleen remains unknown and may also contribute to the phenotypic differences of these tissues.

Conclusions

RASA3 regulates G0/1- Non-G0/1 cell cycle progression in murine HPCs and late erythroblasts. Despite the complexity of comparing BM and spleen erythropoiesis, we can conclude that cell cycle dynamics are associated with the erythropoietic capacity of a tissue. At the time of analysis, *scat* BM erythropoiesis is failing, and *scat* BM HPCs and erythroblasts demonstrate a cell cycle defect, while *scat* spleen is completing temporarily successful stress erythropoiesis and does not demonstrate a cell cycle defect *ex vivo*. This suggests that remodeling of the cell cycle, with a potential role for the microenvironment, is a mechanism of intervention in BM failure. While many questions regarding the role of RASA3 and the *scat* phenotype remain, the identification of two aberrantly cycling populations expands our understanding and allows us to focus future studies on these populations. Such work could further elucidate the RASA3-RAS-cell cycle axis in murine hematopoiesis and erythropoiesis, offering insight into processes with broad disease relevance. Importantly, this data supports the paradigm that targetable processes key to effective hematopoiesis, such as the cell cycle, have layers of regulation yet to be discovered that may have implications for human hematopoietic disease.

Supplementary Material

Refer to Web version on PubMed Central for supplementary material.

Funding

This work is supported by NIH grants HL134043 (LLP), HL144436 (to LB) and HL152099 (to TAK and LB). LB is the recipient of a St. Baldrick's Scholar Award.

References

1. McLean E, et al., Worldwide prevalence of anaemia, WHO Vitamin and Mineral Nutrition Information System, 1993–2005. Public Health Nutr, 2009 12(4): p. 444–54. [PubMed: 18498676]
2. Hattangadi SM, et al., From stem cell to red cell: regulation of erythropoiesis at multiple levels by multiple proteins, RNAs, and chromatin modifications. Blood, 2011 118(24): p. 6258–68. [PubMed: 21998215]
3. Pop R, et al., A key commitment step in erythropoiesis is synchronized with the cell cycle clock through mutual inhibition between PU.1 and S-phase progression. PLoS Biol, 2010 8(9).
4. Tusi BK, et al., Population snapshots predict early haematopoietic and erythroid hierarchies. Nature, 2018 555(7694): p. 54–60. [PubMed: 29466336]
5. Gnanapragasam MN, et al., EKLF/KLF1-regulated cell cycle exit is essential for erythroblast enucleation. Blood, 2016 128(12): p. 1631–41. [PubMed: 27480112]
6. Hara H and Ogawa M, Erythropoietic precursors in mice under erythropoietic stimulation and suppression. Exp Hematol, 1977 5(2): p. 141–8. [PubMed: 844518]
7. Iscove NN, The role of erythropoietin in regulation of population size and cell cycling of early and late erythroid precursors in mouse bone marrow. Cell Tissue Kinet, 1977 10(4): p. 323–34. [PubMed: 884703]

8. Li X, et al., Fanconi anemia type C-deficient hematopoietic stem/progenitor cells exhibit aberrant cell cycle control. Blood, 2003 102(6): p. 2081–4. [PubMed: 12763929]
9. Sankaran VG, et al., Cyclin D3 coordinates the cell cycle during differentiation to regulate erythrocyte size and number. Genes Dev, 2012 26(18): p. 2075–87. [PubMed: 22929040]
10. Sankaran VG, Orkin SH, and Walkley CR, Rb intrinsically promotes erythropoiesis by coupling cell cycle exit with mitochondrial biogenesis. Genes Dev, 2008 22(4): p. 463–75. [PubMed: 18258751]
11. Vlachos A, Blanc L, and Lipton JM, Diamond Blackfan anemia: a model for the translational approach to understanding human disease. Expert Rev Hematol, 2014 7(3): p. 359–72. [PubMed: 24665981]
12. Wegman-Ostrosky T and Savage SA, The genomics of inherited bone marrow failure: from mechanism to the clinic. Br J Haematol, 2017 177(4): p. 526–542. [PubMed: 28211564]
13. Ashley RJ, et al., Steroid resistance in Diamond Blackfan anemia associates with p57Kip2 dysregulation in erythroid progenitors. J Clin Invest, 2020 130(4): p. 2097–2110. [PubMed: 31961825]
14. Hwang Y, et al., Global increase in replication fork speed during a p57(KIP2)-regulated erythroid cell fate switch. Sci Adv, 2017 3(5): p. e1700298. [PubMed: 28560351]
15. Blanc L, et al., Critical function for the Ras-GTPase activating protein RASA3 in vertebrate erythropoiesis and megakaryopoiesis. Proc Natl Acad Sci U S A, 2012 109(30): p. 12099–104. [PubMed: 22773809]
16. Hartman ES, et al., Increased Reactive Oxygen Species and Cell Cycle Defects Contribute to Anemia in the RASA3 Mutant Mouse Model scat. Front Physiol, 2018 9: p. 689. [PubMed: 29922180]
17. Flygare J, et al., HIF1alpha synergizes with glucocorticoids to promote BFU-E progenitor self-renewal. Blood, 2011 117(12): p. 3435–44. [PubMed: 21177435]
18. Koulnis M, et al., Identification and analysis of mouse erythroid progenitors using the CD71/TER119 flow-cytometric assay. J Vis Exp, 2011(54).
19. Robledo RF, et al., Differential Effects of RASA3 Mutations on Hematopoiesis are Profoundly Influenced by Genetic Background and Molecular Variant. PLos Genetics, 2020 In Press.
20. Love MI, Huber W, and Anders S, Moderated estimation of fold change and dispersion for RNA-seq data with DESeq2. Genome Biol, 2014 15(12): p. 550. [PubMed: 25516281]
21. Spangrude GJ and Brooks DM, Mouse strain variability in the expression of the hematopoietic stem cell antigen Ly-6A/E by bone marrow cells. Blood, 1993 82(11): p. 3327–32. [PubMed: 8241503]
22. Jassal B, et al., The reactome pathway knowledgebase. Nucleic Acids Res, 2020 48(D1): p. D498–D503. [PubMed: 31691815]
23. Liu J, et al., Quantitative analysis of murine terminal erythroid differentiation in vivo: novel method to study normal and disordered erythropoiesis. Blood, 2013 121(8): p. e43–9. [PubMed: 23287863]
24. Chen L, et al., Dynamic Changes in Murine Erythropoiesis from Birth to Adulthood: Implications for the Study of Murine Models of Anemia. Blood Advances, 2020 In Press.
25. Dulmovits BM, et al., Characterization, regulation, and targeting of erythroid progenitors in normal and disordered human erythropoiesis. Curr Opin Hematol, 2017 24(3): p. 159–166. [PubMed: 28099275]
26. Malumbres M and Pellicer A, RAS pathways to cell cycle control and cell transformation. Front Biosci, 1998 3: p. d887–912. [PubMed: 9696882]
27. Li FX, et al., Defective gene expression, S phase progression, and maturation during hematopoiesis in E2F1/E2F2 mutant mice. Mol Cell Biol, 2003 23(10): p. 3607–22. [PubMed: 12724419]
28. Dimri GP, et al., Regulation of a senescence checkpoint response by the E2F1 transcription factor and p14(ARF) tumor suppressor. Mol Cell Biol, 2000 20(1): p. 273–85. [PubMed: 10594030]
29. Boultwood J and Wainscoat JS, Gene silencing by DNA methylation in haematological malignancies. Br J Haematol, 2007 138(1): p. 3–11. [PubMed: 17489980]

30. Iolascon A, et al., Congenital dyserythropoietic anemias: molecular insights and diagnostic approach. Blood, 2013 122(13): p. 2162–6. [PubMed: 23940284]

31. Hirota T, et al., Aurora-A and an interacting activator, the LIM protein Ajuba, are required for mitotic commitment in human cells. Cell, 2003 114(5): p. 585–98. [PubMed: 13678582]

32. Johnson EO, et al., PHLDA1 is a crucial negative regulator and effector of Aurora A kinase in breast cancer. J Cell Sci, 2011 124(Pt 16): p. 2711–22. [PubMed: 21807936]

33. Dynlacht BD, Regulation of transcription by proteins that control the cell cycle. Nature, 1997 389(6647): p. 149–52. [PubMed: 9296491]

34. Jensen LJ, et al., Co-evolution of transcriptional and post-translational cell-cycle regulation. Nature, 2006 443(7111): p. 594–7. [PubMed: 17006448]

35. Spike BT, et al., The Rb tumor suppressor is required for stress erythropoiesis. EMBO J, 2004 23(21): p. 4319–29. [PubMed: 15457215]

36. Paulson RF, Shi L, and Wu DC, Stress erythropoiesis: new signals and new stress progenitor cells. Curr Opin Hematol, 2011 18(3): p. 139–45. [PubMed: 21372709]

Highlights:

1. RASA3 has a biphasic role in regulating the cell cycle during murine erythropoiesis
2. *Scat* offers insights into cell cycle regulation during murine erythropoiesis.

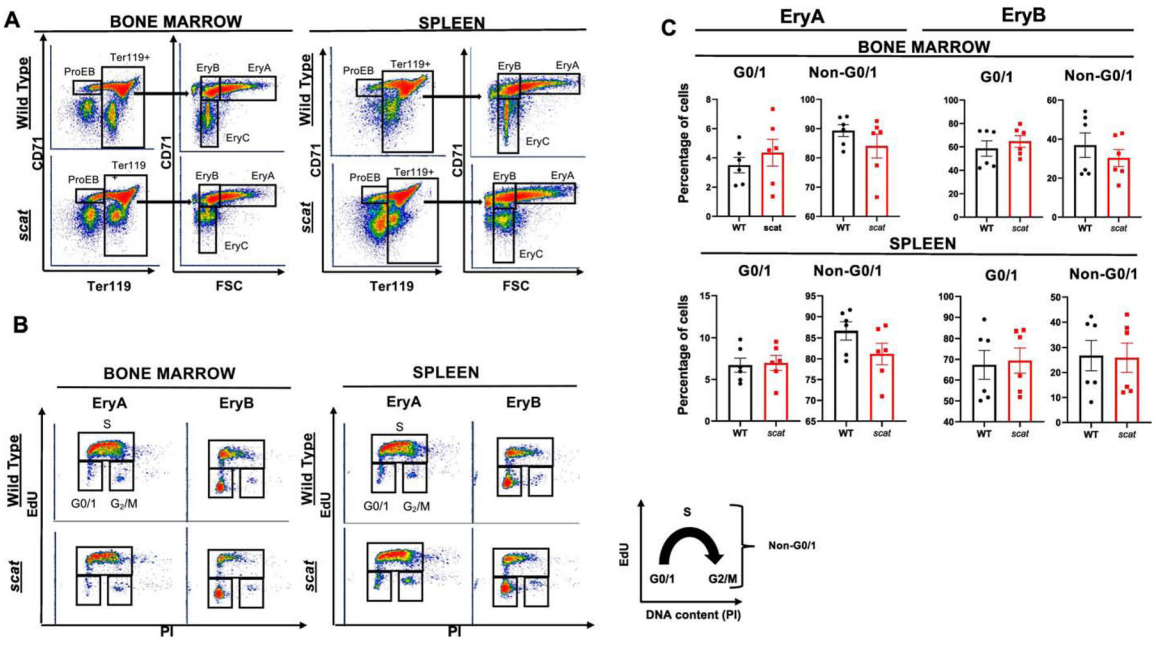

Figure 1. *scat* crisis erythroblasts demonstrate a cell cycle defect that aligns with delayed terminal differentiation.

(A) *scat* BM and spleen-derived erythroblasts demonstrate a delay in terminal erythroid differentiation at the EryB/EryC transition compared to WT; (B) cell cycle analyses using EdU and PI (inset diagram) of *scat* versus WT erythroblast populations, (C) *scat* EryA and EryB demonstrate a trend of accumulation in G0/G1 and failed progression to S-phase compared to WT, most notable in the BM; (n=6).

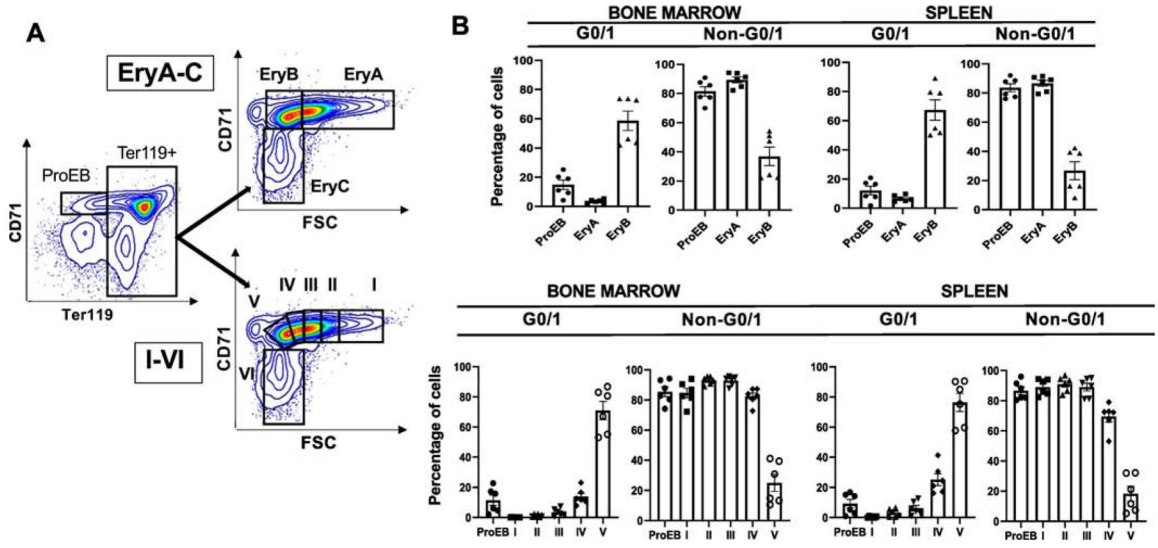

Figure 2. Cell cycle profiles of late erythroblasts are further resolved by simultaneous changes in cell size and CD71 expression.

(A) Representative adapted gating of Ter119^{+} erythroblasts by progressively decreasing cell size and subsequently decreasing CD71 expression yields resolution of EryA into populations I, II, and III, EryB into populations IV and V, with EryC reticulocytes and erythrocytes represented by population VI. (B) Quantified cell cycle analyses of WT bone marrow and spleen-derived erythroblast populations by both gating schemes demonstrates an initial small increase in cycling from proerythroblasts to later stages, followed by accumulation in G0/1 with progressive differentiation. Comparison of EryA-C (top) and I-VI (bottom) gating strategies reveals that cell cycle patterns of EryA contain the relatively uniform cycling profiles of I, II, and II, while cell cycle patterns of EryB, at the intersection of changes in cell size and CD71 expression, are a more heterogeneous combination of populations IV and V. These patterns are conserved across BM and spleen.

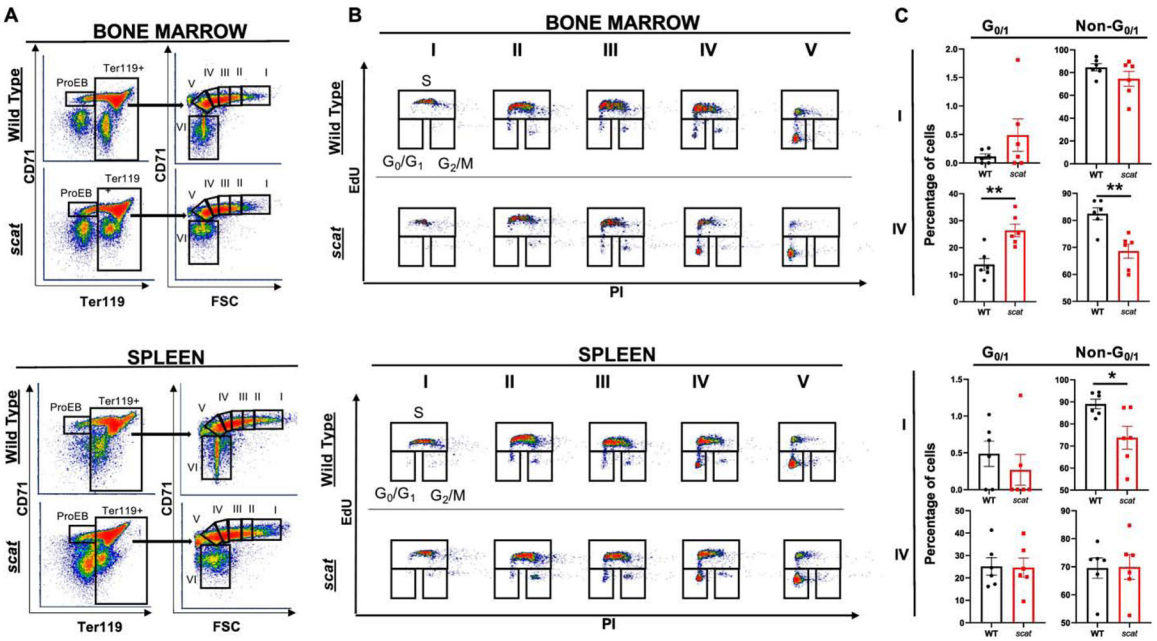

Figure 3. The cell cycle defect in *scat* can be resolved to a specific late erythroblast population in BM.

(A) *scat* vs WT BM and spleen erythroblast populations resolved by I-VI gating, (B) comparative cell cycle analyses of populations I-V in *scat* vs WT quantified in (C) reveal G0/1 accumulation and decreased cell cycle progression in BM population IV, while the spleen demonstrates less notable decreased cell cycle progression in population I and normal cycling in population IV. *p<0.05, **p<0.01 WT vs *Scat*, unpaired t-test (n=6)

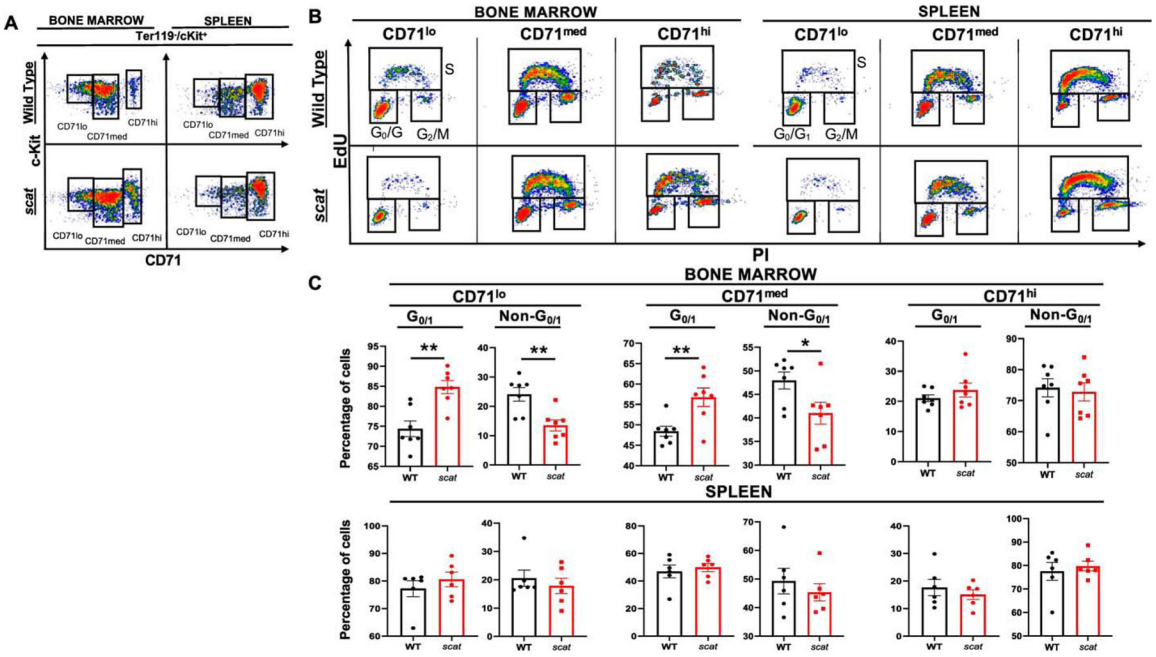

Figure 4. *scat* hematopoietic progenitors in the BM, but not in the spleen, demonstrate a cell cycle defect.

(A) Gating of lineage-depleted, c-KIT+ BM and spleen cells by CD71 expression demonstrating patterns of hematopoietic progenitor differentiation in WT and *scat* BM and spleen; (B) Representative cell cycle analyses of these populations, quantified in (C), demonstrating G0/1 accumulation and decreased cell cycle progression in *scat* BM CD71lo/med populations, with normal cycling in *scat* BM CD71hi cells, and normal cell cycling in all *scat* spleen progenitor populations compared to WT. *p<0.05, **p<0.01 WT vs *Scat*, unpaired t-test (BM, n=7; spleen, n=6).

Table 1.

The top five Reactome pathways represented by differentially expressed gene lists in bone marrow SMP and MEP comparisons of *scat* crisis vs WT and *scat* crisis vs. *scat* partial remission.

Only the BM MEP gene list upregulated in *scat* crisis vs. *scat* partial remission demonstrates enrichment of a cell cycle pathway. Also of note given the role of RASA3 as a regulator of RAS, signaling by MAPK mutants is an enriched pathway in BM SMP upregulated genes in *scat* crisis vs. WT and BM MEP upregulated genes in *scat* crisis vs. *scat* partial remission.

Bone Marrow SMP		**Bone Marrow MEP**	
↓ *scat* crisis vs WT	↓ *scat* crisis vs partial remission	↓ *scat* crisis vs WT	↓ *scat* crisis vs partial remission
HCN channels	Attenuation phase	UNC93B1 deficiency-HSE	Attenuation phase
Cam-PDE 1 activation	HSF1-dependent transactivation	MET interacts with TNS proteins	HSF1-dependent transactivation
cGMP effects	Regulation of HSF1-mediated heat shock response	NFG and proNGF binds to p75NTR	Regulation of HSF1-mediated heat shock response
PKB-mediated events	Cellular response to heat stress	Regulation of gap junction activity	Cellular response to heat stress
PDE3B signaling	HSF1 activation	Axonal growth stimulation	HSF1 activation
↑ *scat* crisis vs WT	↑ *scat* crisis vs partial remission	↑ *scat* crisis vs WT	↑ *scat* crisis vs partial remission
Metallothioneins bind metals	Metallothioneins bind metals	Metallothioneins bind metals	Activation of PUMA and translocation to mitochondria
Response to metal ions	Nuclear receptor transcription pathway	Response to metal ions	Activation of BH3-only proteins
Defective RHAG causes regulator type Rh-null hemolytic anemia (RHN)	Response to metal ions	RUNX1 regulates expression of components of tight junctions	Resistance of ERBB2 KD mutants to: lapatinib, AEE788, trastuzumab, tesevatinib, afatinib, neratinib, sapitinib, Osimertinib
ABC transporters in lipid homeostasis	Defective RHAG causes regulator type Rh-null hemolytic anemia (RHN)	IL-7 signaling	**TP53 regulates transcription of additional cell cycle genes whose exact role in the p53 pathway remain uncertain**
Signaling by MAPK mutants	Defective B3GALTL causes Peters-plus syndrome (PpS)	IRS activation	Signaling by MAPK mutants

Table 2.

The top five Reactome pathways represented by differentially expressed gene lists in spleen SMP and MEP comparisons of *scat* crisis vs WT and *scat* crisis vs. *scat* partial remission.

No spleen SMP or MEP comparison gene lists demonstrates enrichment of a cell cycle pathway. Also of note given the role of RASA3 as a regulator of RAS, signaling by MAPK mutants is an enriched pathway in spleen SMP upregulated genes in *scat* crisis vs. *scat* partial remission.

Spleen SMP		**Spleen MEP**	
↓ *scat* crisis vs WT	↓ *scat* crisis vs partial remission	↓ *scat* crisis vs WT	↓ *scat* crisis vs partial remission
Scavenging by Class H Receptors	Defective CYP7B1 causes spastic paraplegia 5A, autosomal recessive (SPG5A) and congenital bile acid synthesis defect 3 (CBAS3)	Prostanoid ligand receptors	Neutrophil degranulation
RUNX3 regulates immune response and cell migration	Neurexins and neuroligins	Neutrophil degranulation	Molecules associated with elastic fibres
Classical antibody-mediated complement activation	Muscarinic acetylcholine receptors	Collagen chain trimerization	Defective LFNG causes SCDO3
MyD88 deficiency (TLR5)	FGFR1b ligand binding and activation	Laminin interactions	RAB geranylgeranylation
Creation of C4 and C2 activators	Abacavir transmembrane transport	CD22 mediated BCR regulation	Abacavir transmembrane transport
↑ scat crisis vs WT	↑ scat crisis vs partial remission	↑ scat crisis vs WT	↑ scat crisis vs partial remission
Rhesus blood group biosynthesis	HS-GAG biosynthesis	Interleukin-4 and Interleukin-13 signaling	Interleukin-4 and interleukin-13 signaling
Metallothioneins bind metals	Metallothioneins bind metals	RUNX1 regulates transcription of genes involved in differentiation of keratinocytes	Degradation of extracellular matrix
Effects of PIP2 hydrolysis	Response to metal ions	Metallothioneins bind metals	Activation of matrix metalloproteinases
Response to metal ions	Intestinal infectious disease	Senescence-associated secretory phenotype (SASP)	Collagen degradation
Defective RHAG causes regulator type Rh-null hemolytic anemia	Signaling by MAPK mutants	Response to metal ions	Expression and processing of neurotrophins

Tables 3.

Analysis of all population comparisons for enrichment of cell cycle pathways yields similar signatures in BM and Spleen MEP in *scat* crisis vs. *scat* partial remission.

All population comparison gene lists were analyzed for cell cycle pathway enrichments with $p<0.05$ by the Reactome pathway database. No SMP comparisons in BM or spleen had cell cycle enrichment. Within the MEP, similar enrichment for G1-S checkpoint related processes was identified in BM and spleen in *scat* crisis vs. *scat* partial remission, with BM MEP *scat* crisis vs. WT also showing enrichment for PHLDA1 and AURKA interaction in downregulated genes.

Bone Marrow MEP	
↓ *scat* crisis vs WT	↓ *scat* crisis vs partial remission
Interaction between PHLDA1 and AURKA	Interaction between PHLDA1 and AURKA
↑ *scat* crisis vs WT	Evasion of oxidative stress induced senescence due to $p14^{ARF}$ defects
0 cell cycle terms	Evasion of oncogene induced senescence due to $p14^{ARF}$ defects
	↑ *scat* crisis vs partial remission
	Aberrant regulation of mitotic G_1-S transition in cancer due to RB1 defects
	Defective binding of RB1 mutants to E2F1 (E2F2, E2F3)
↓ *scat* crisis vs WT	↓ *scat* crisis vs partial remission
0 cell cycle terms	Evasion of oxidative stress induced senescence due to p14ARF defects
↑ scat crisis vs WT	Evasion of oncogene induced senescence due to p14ARF defects
0 cell cycle terms	↑ scat crisis vs partial remission
	Aberrant regulation of mitotic G1-S transition in cancer due to RB1 defects
	Defective binding of RB1 mutants to E2F1 (E2F2, E2F3)